

MULTIGAP DIFFRACTION AT CDF <sup>a</sup>

K. GOULIANOS

*The Rockefeller University*

*1230 York Avenue, New York, NY 10021, USA*

*(For the CDF Collaboration)*



We present a study of  $\bar{p}p$  collisions with a leading antiproton and a rapidity gap in addition to that associated with the antiproton. The second gap is either within the region available to the proton dissociation products,  $\bar{p}+p \rightarrow (\bar{p}+gap)+X+gap+Y$ , or adjacent to the outgoing proton  $\bar{p}+p \rightarrow (\bar{p}+gap)+X+(gap+p)$ . Results are reported for two-gap to one-gap event ratios and compared with one-gap to no-gap ratios and with theoretical expectations.

Diffractive  $\bar{p}p$  interactions are characterized by a leading (high longitudinal momentum) outgoing proton or antiproton and/or a large *rapidity gap*, defined as a region of pseudorapidity,  $\eta \equiv -\ln \tan \frac{\theta}{2}$ , devoid of particles. The large rapidity gap is presumed to be due to the exchange of a Pomeron, which carries the internal quantum numbers of the vacuum. Rapidity gaps formed by multiplicity fluctuations in non-diffractive (ND) events are exponentially suppressed with  $\Delta\eta$ , so that gaps of  $\Delta\eta > 3$  are almost purely diffractive. At high energies, where the available rapidity space is large, diffractive events may have more than one large gap. Using the Collider Detector at Fermilab (CDF), we have studied two types of events with two diffractive rapidity gaps in an event, shown schematically in Figs. 1 and 2.

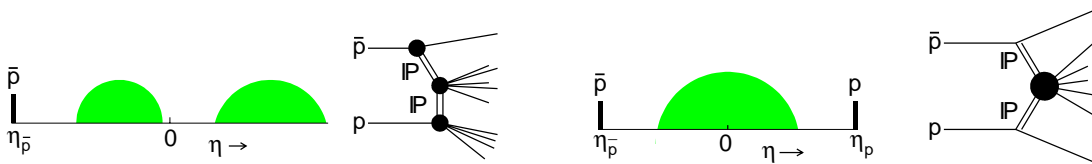


Fig. 1: Single  $\oplus$  Double Diffraction (SDD)      Fig. 2: Double Pomeron Exchange (DPE)

<sup>a</sup>Presented at XXXVII<sup>th</sup> Rencontres de Moriond, Les Arcs, Savoie, France, March 16-23, 2002.

The motivation for this study is its potential for providing further understanding of the underlying mechanism responsible for the suppression of diffractive cross sections at high energies relative to Regge theory predictions. As shown in Figs. 3 and 4, such a suppression has been observed for both single diffraction (SD),  $\bar{p}(p) + p \rightarrow [\bar{p}(p) + gap] + X$ , and double diffraction (DD),  $\bar{p}(p) + p \rightarrow X_1 + gap + X_2$ .

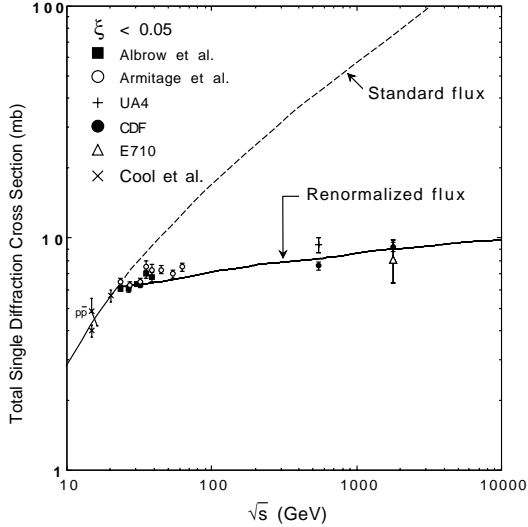


FIG. 3: The  $\bar{p}p$  total SD cross section exhibits an  $s$ -dependence consistent with the renormalization procedure of Ref. <sup>1</sup>, contrary to the  $s^{2\epsilon}$  behaviour expected from Regge theory (figure from Ref. <sup>1</sup>).

Naively, the suppression relative to Regge based predictions is attributed to the spoiling of the diffractive rapidity gap by color exchanges in addition to Pomeron exchange. In an event with two rapidity gaps, additional color exchanges would generally spoil both gaps. Hence, ratios of two-gap to one-gap rates should be unsuppressed. Measurements of such ratios could therefore be used to test the QCD aspects of gap formation without the complications arising from the rapidity gap survival probability.

The data used for this study are inclusive SD event samples at  $\sqrt{s} = 1800$  and 630 GeV collected by triggering on a leading antiproton detected in a Roman Pot Spectrometer (RPS)<sup>4,5</sup>. Below, we list the number of events used in each analysis within the indicated regions of antiproton fractional momentum loss  $\xi_{\bar{p}}$  and 4-momentum transfer squared  $t$ , after applying the vertex cuts  $|z_{vtx}| < 60$  cm and  $N_{vtx} \leq 1$  and a 4-momentum squared cut of  $|t| < 0.02$  GeV<sup>2</sup> (except for DPE at 1800 GeV for which  $|t| < 1.0$  GeV<sup>2</sup>):

Process	$\xi$	Events at 1800 GeV	Events at 630 GeV
SDD	$0.06 < \xi < 0.09$	412K	162K
DPE	$0.035 < \xi < 0.095$	746K	136K

In the SDD analysis, the mean value of  $\xi = 0.07$  corresponds to a diffractive mass of  $\approx 480$  (170) GeV at  $\sqrt{s} = 1800$  (630) GeV. The diffractive cluster X in such events covers almost the entire CDF calorimetry, which extends through the region  $|\eta| < 4.2$ . Therefore, we use the same method of analysis as that used to extract the gap fraction in the case of DD<sup>3</sup>. We search for *experimental gaps* overlapping  $\eta = 0$ , defined as regions of  $\eta$  with no tracks or calorimeter towers above thresholds chosen to minimize calorimeter noise contributions. The results, corrected for triggering efficiency of  $BBC_p$  (the beam counter array on the proton side) and converted to *nominal gaps* defined by  $\Delta\eta = \ln \frac{s}{M_1^2 M_2^2}$ , are shown in Figs. 5 and 6.

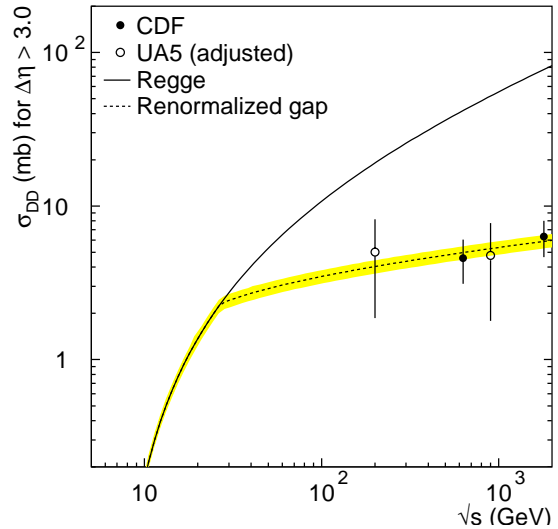


FIG. 4: The  $\bar{p}p$  total DD (central gap) cross section agrees with the prediction of the *renormalized rapidity gap* model<sup>2</sup>, contrary to the  $s^{2\epsilon}$  expectation from Regge theory (figure from Ref. <sup>3</sup>).

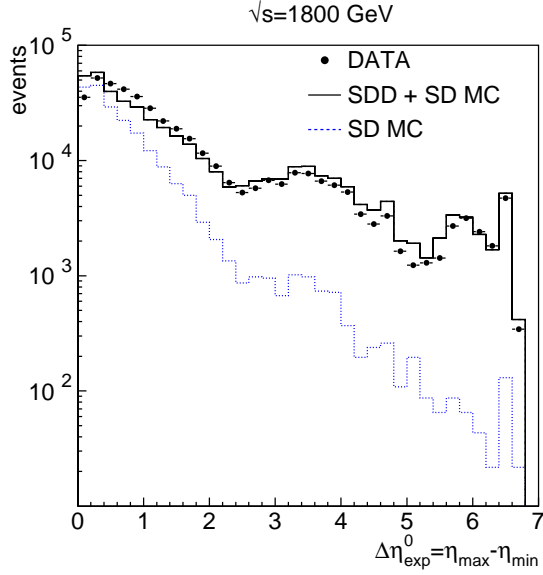


Fig. 5: The number of events as a function of  $\Delta\eta_{exp}^0 = \eta_{max} - \eta_{min}$  for data at  $\sqrt{s} = 1800$  GeV (points), for SDD Monte Carlo generated events (solid line), and for only SD Monte Carlo events (dashed line).

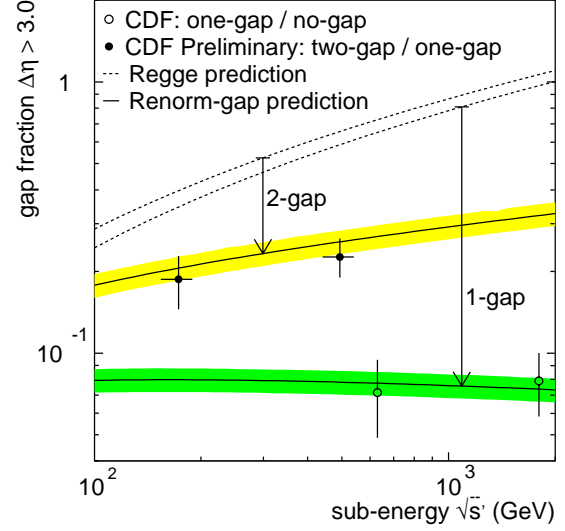


FIG. 6: Ratios of SDD to SD rates (points) and DD to total (no-gap) rates (open circles) as a function of  $\sqrt{s'}$  of the sub-process  $IPp$  and of  $\bar{p}p$ , respectively. The uncertainties are highly correlated among all data points.

The SDD Monte carlo simulation is based on Regge theory Pomeron exchange with the normalization left free to be determined from the data. The differential  $dN/d\Delta\eta^0$  shape agrees with the theory (Fig. 5), but the two-gap to one-gap ratio is suppressed (Fig. 6). However, the suppression is not as large that as in the one-gap to no-gap ratio. The bands through the data points represent predictions of the renormalized multigap parton model approach to diffraction<sup>6</sup>, which is a generalization of the renormalization models used for single<sup>1</sup> and double<sup>2</sup> diffraction.

In the DPE analysis, the  $\xi_p$  is measured from calorimeter and beam counter information using the formula below and summing over all particles, defined experimentally as beam-beam counter (BBC) hits or calorimeter towers above  $\eta$ -dependent thresholds chosen to minimize noise contributions.

$$\xi_p^X = \frac{M_X^2}{\xi_{\bar{p}} \cdot s} = \frac{\sum_i E_T^i \exp(+\eta^i)}{\sqrt{s}}$$

For BBC hits we use the average value of  $\eta$  of the BBC segment of the hit and an  $E_T$  value randomly chosen from the expected  $E_T$  distribution. The  $\xi^X$  obtained by this method was calibrated by comparing  $\xi_p^X$ , obtained by using  $\exp(-\eta^i)$  in the above equation, with the value of  $\xi_{\bar{p}}^{RPS}$  measured by the Roman Pot Spectrometer.

Figure 7 shows the  $\xi_p^X$  distribution for  $\sqrt{s} = 1800$  GeV. The bump at  $\xi_p^X \sim 10^{-3}$  is attributed to central calorimeter noise and is reproduced in Monte Carlo simulations. The variation of tower  $E_T$  threshold across the various components of the CDF calorimetry does not affect appreciably the slope of the  $\xi_p^X$  distribution. The solid line represents the distribution measured in SD<sup>7</sup>. The shapes of the DPE and SD distributions are in good agreement all the way down to the lowest values kinematically allowed.

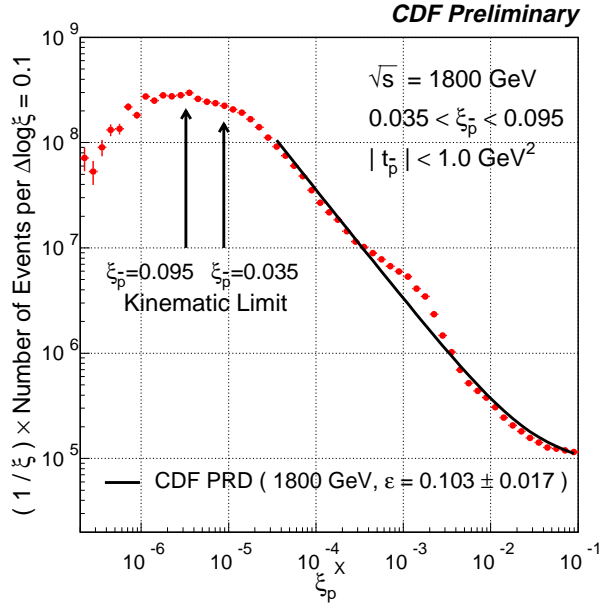


Fig. 7:  $\xi_{\bar{p}}^X$  distribution at  $\sqrt{s} = 1800$  GeV for events with a  $\bar{p}$  of  $0.035 < \xi_{\bar{p}}^{RPS} < 0.095$ . The solid line is the distribution obtained in single diffraction dissociation. The bump at  $\xi_{\bar{p}}^X \sim 10^{-3}$  is due to central calorimeter noise and is reproduced in Monte Carlo simulations.

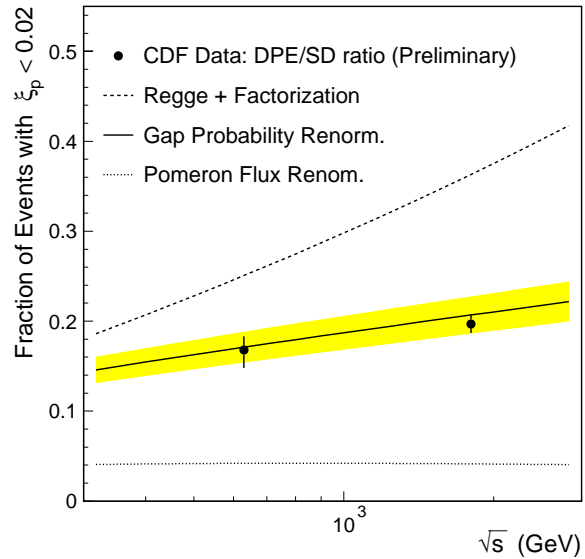


FIG. 8: Measured ratios of DPE to SD rates (points) compared with predictions based on Regge theory (dashed), Pomeron flux renormalization for both exchanged Pomerons (dotted) and gap probability renormalization (solid line).

The ratio of DPE to inclusive SD events was evaluated for  $\xi_p^X < 0.02$ . The results for  $\sqrt{s} = 1800$  and 630 GeV are presented in the table below and in Fig. 8. Also presented are the expectations from gap probability renormalization<sup>6</sup>, Regge theory and factorization, and Pomeron flux renormalization for both exchanged Pomerons<sup>1</sup>. The quoted uncertainties are largely systematic for both data and theory; the theoretical uncertainties of 10% are due to the uncertainty in the ratio of the triple-Pomeron to the Pomeron-nucleon couplings<sup>8</sup>. The data are in excellent agreement with the predictions of the gap renormalization approach.

Source	$R_{SD}^{DPE}(1800 \text{ GeV})$	$R_{SD}^{DPE}(630 \text{ GeV})$
Data	$0.197 \pm 0.010$	$0.168 \pm 0.018$
$P_{gap}$ renormalization	$0.21 \pm 0.02$	$0.17 \pm 0.02$
Regge $\oplus$ factorization	$0.36 \pm 0.04$	$0.25 \pm 0.03$
$IP$ -flux renormalization	$0.041 \pm 0.004$	$0.041 \pm 0.004$

## References

1. K. Goulianos, Phys. Lett. **B358**, 379 (1995); **B363**, 268 (1995).
2. K. Goulianos, arXiv:hep-ph/9806384.
3. T. Affolder *et al.*, CDF Collaboration, Phys. Rev. Lett. **87**, 141802 (2001).
4. T. Affolder *et al.*, CDF Collaboration, Phys. Rev. Lett. **84**, 5083 (2000).
5. D. Acosta *et al.*, CDF Collaboration, Phys. Rev. Lett. **88**, 151802 (2002).
6. K. Goulianos, hep-ph/0110240; hep-ph/0203141.
7. F. Abe *et al.*, Phys. Rev. **D 50** (1994) 5535.
8. K. Goulianos and J. Montanha, Phys. Rev. **D50**, 114017 (1999).